

# SynchroLoad Push-Out Experiments



Stefan Bruns<sup>\*,1</sup>, Julian Moosmann<sup>2</sup>, Diana Krüger<sup>1</sup>, Silvia Galli<sup>3</sup>, Jörg Hammel<sup>2</sup>, Florian Wieland<sup>1</sup>, Berit Zeller-Plumhoff<sup>1</sup>, Regine Willumeit-Römer<sup>1</sup>

<sup>1</sup> Institute of Metallic Biomaterials; <sup>2</sup> Institute of Materials Physics; <sup>3</sup> University of Malmö, Faculty of Odontology

## Abstract

SynchroLoad performs a material-dependent characterization of the **biomechanical properties of bone-screw implant systems**. For this purpose rat tibiae were implanted with screws made of **titanium, PEEK and bioresorbable magnesium alloys** and explants were acquired after **varying healing periods**. We performed **push-out experiments** with the explants using a custom loading cell, enabling the **in situ monitoring** of the experiment with **synchrotron  $\mu$ -CT** at beamline P05 (DESY). The strain uptake in the bone samples was evaluated on the voxel level with a custom built high-performance variational solver for **digital volume correlation**. The combination of a mechanical test with 4D imaging enabled us to consider implant stability in the context of bone morphology and strain distribution.

## Experimental Setup

### Samples

- 42 rat tibiae implanted with **1.9 mm o.d. screws**
- implant materials: **titanium, PEEK, Mg-10Gd, Mg-5Gd**
- healing period: **4 weeks, 8 weeks, 12 weeks**

### $\mu$ -CT

- beamline P05 at PETRA III (DESY)
- absorption contrast @ 40 keV
- 1.3  $\mu$ m detector pixel resolution, **5.3  $\mu$ m spatial resolution**
- radiation dose calculated to leave **collagen unaffected for at least 10 scans**
- 1200 projection @ 34 ms exposure

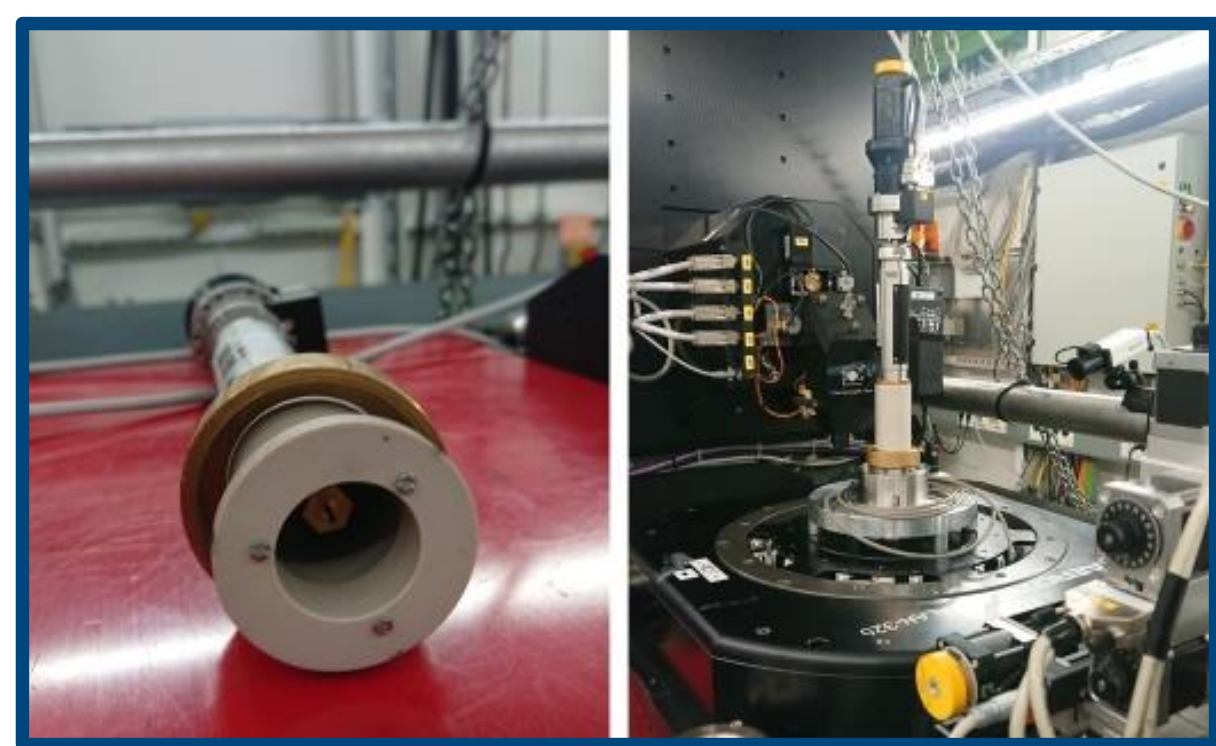


Figure 2: Beamline setup with custom loading cell (left panel) and loading cell mounted on a rotary table in front of the detector (right panel).

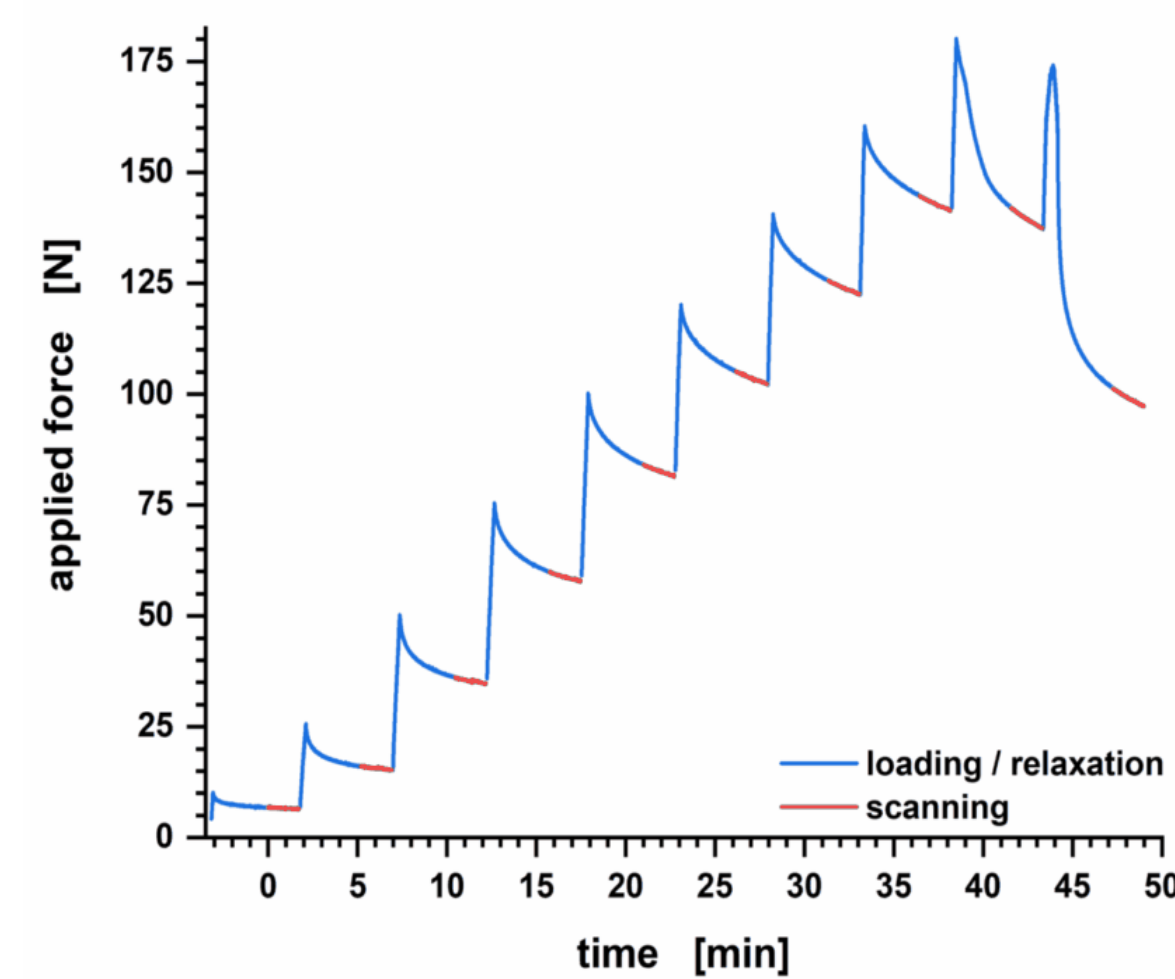


Figure 3: Exemplary pressure profile of a push-out experiment. Load was increased incrementally (blue) and samples were left to relax for 3 minutes before scanning (red).

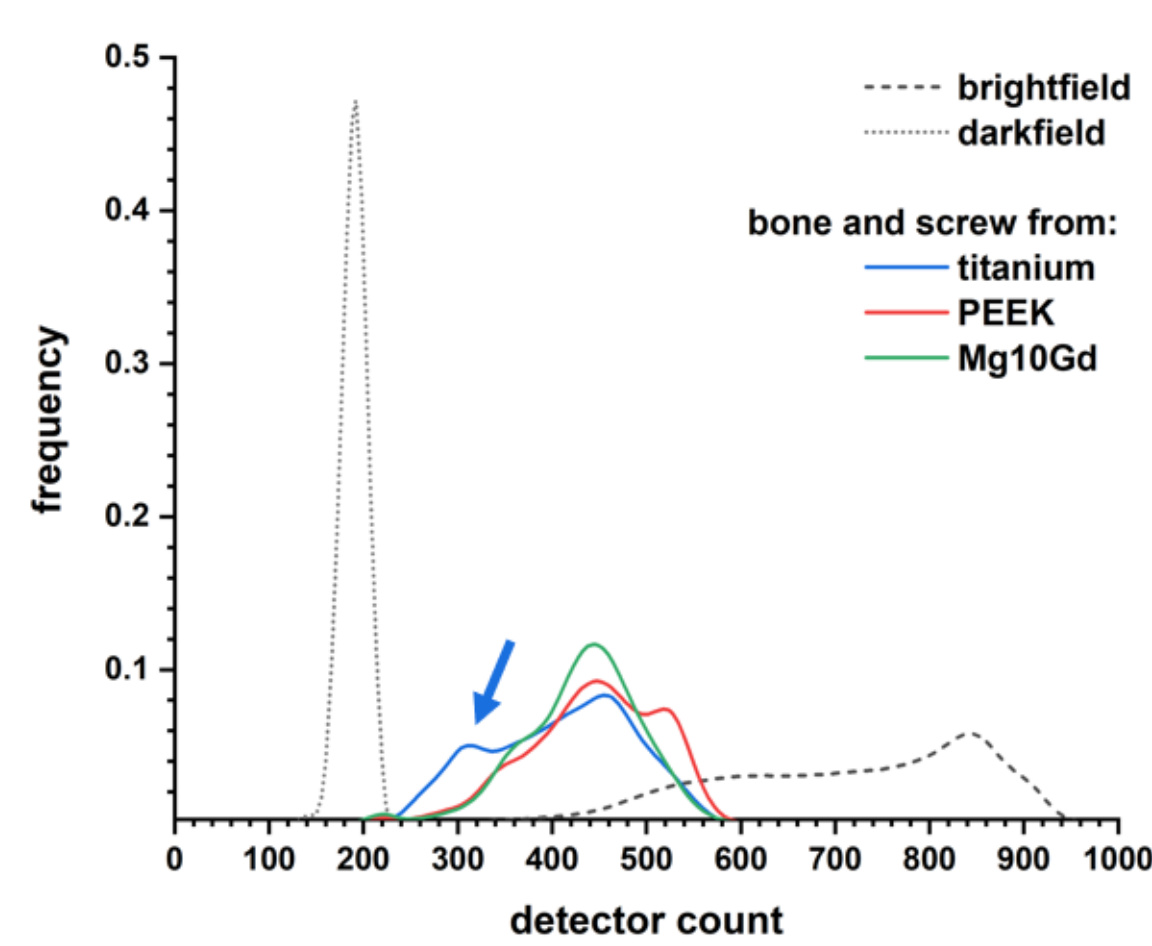
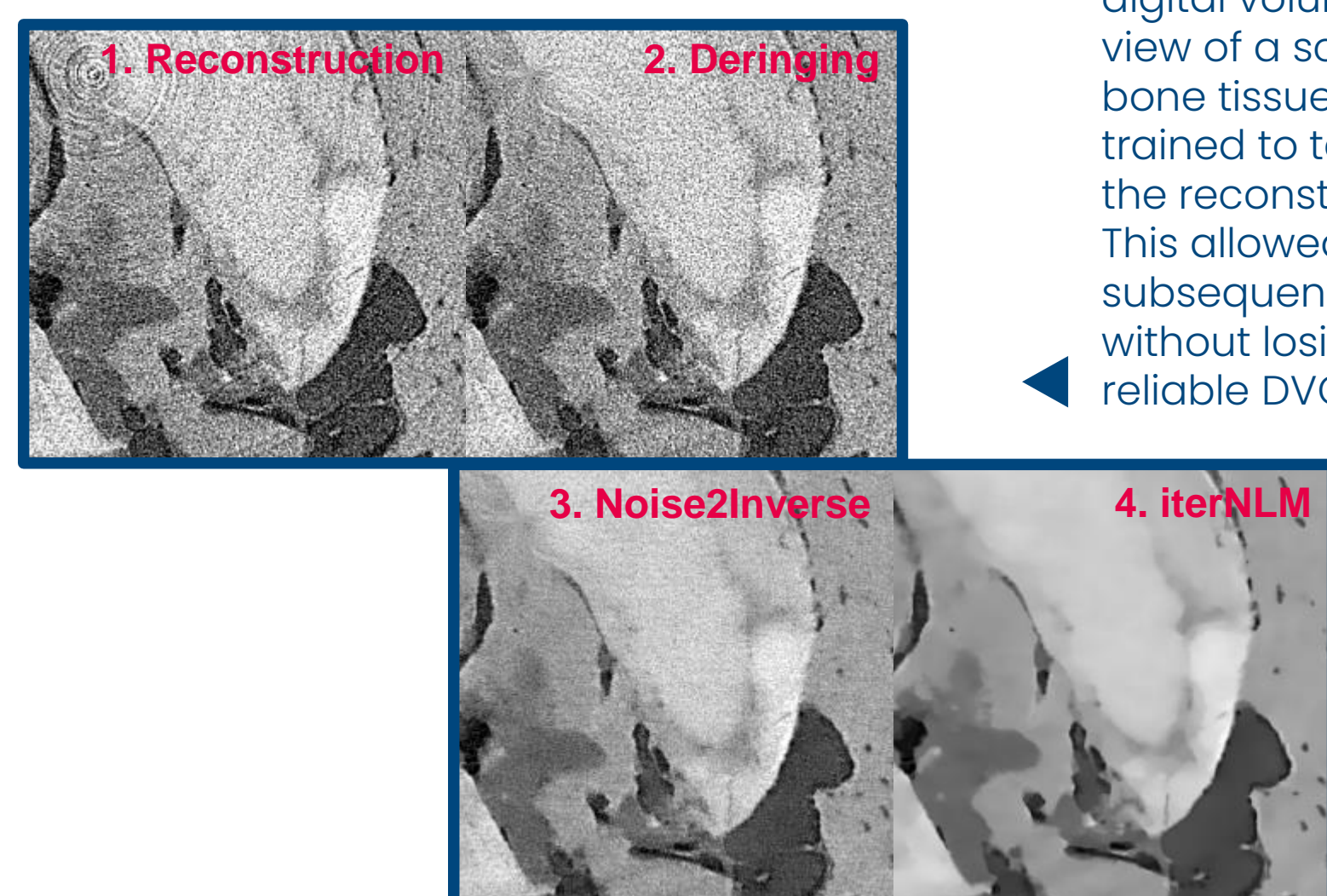


Figure 4: Photon counts at the detector with a bone-screw system using titanium (blue), PEEK (red) or Mg-10Gd (green) as an implant material. Counts were especially low with titanium due to dose considerations resulting in increased noise levels and pronounced reconstruction artefacts. The latter need to be handled rigorously to avoid biases in the DVC analysis.

Figure 5: Outline of the applied image restoration procedure before morphological analysis and digital volume correlation (DVC) with a 2D detail view of a scanned Mg-10Gd implant surrounded by bone tissue. After deringing a neural network was trained to target the random noise component in the reconstructions via Noise2Inverse algorithm. This allowed eliminating textured artifacts in a subsequent iterative non-local means filtering step without losing details in the structure required for reliable DVC.



## Conclusions

Implant materials affect both morphology and strain transfer in the peri-implant region in a characteristic manner. Differences between materials are more pronounced than with extended healing periods. One resulting implication is that there is **not a single morphological descriptor correlating with implant stability**. Correlations in our data suggest that the implant stability with titanium benefits from implantation depth, with PEEK from initially thick cortical bone and with resorbable implants from available surface area.

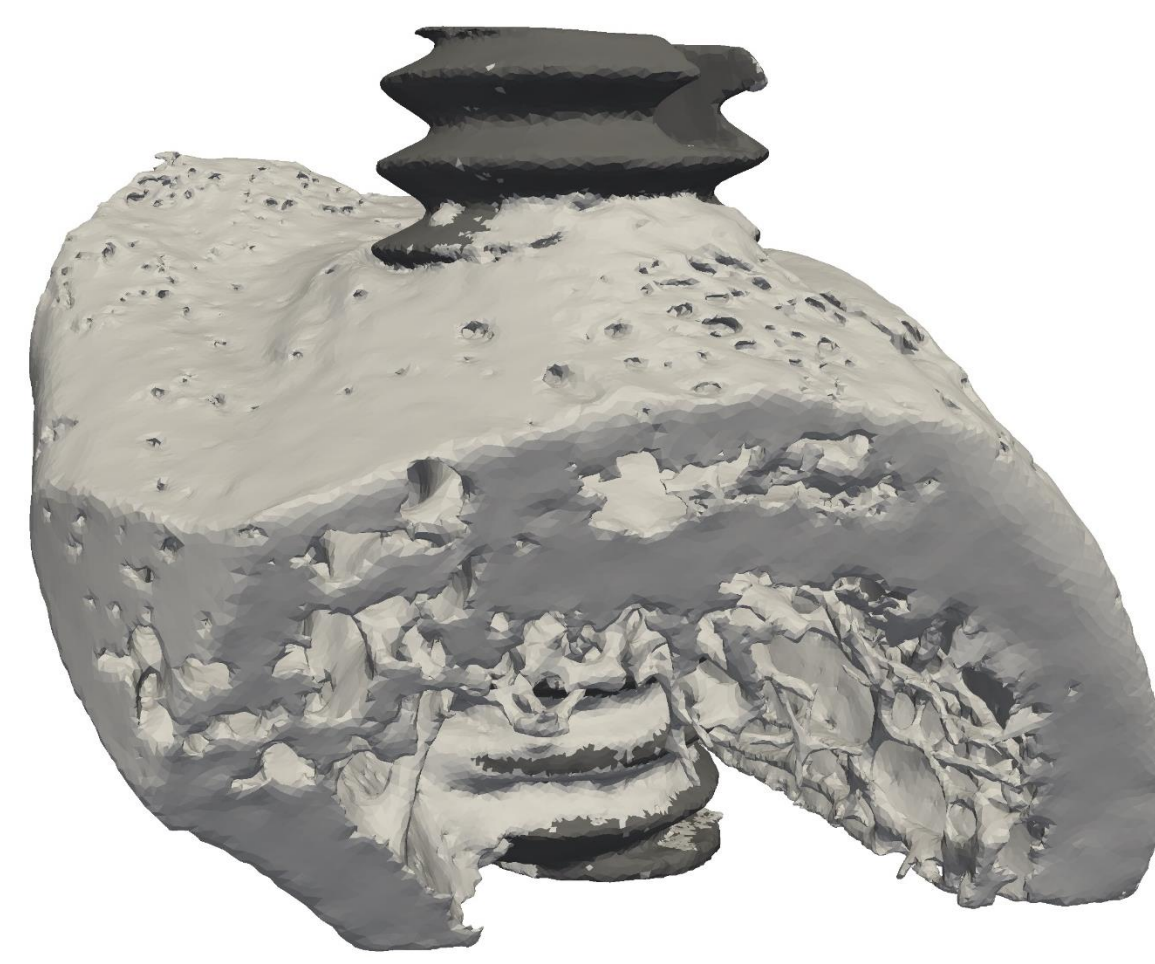


Figure 1: Exemplary rendering of one of the bone-screw implant systems tested showing a rat femur implanted with a titanium screw after 12 weeks of healing.

## Implant Stability

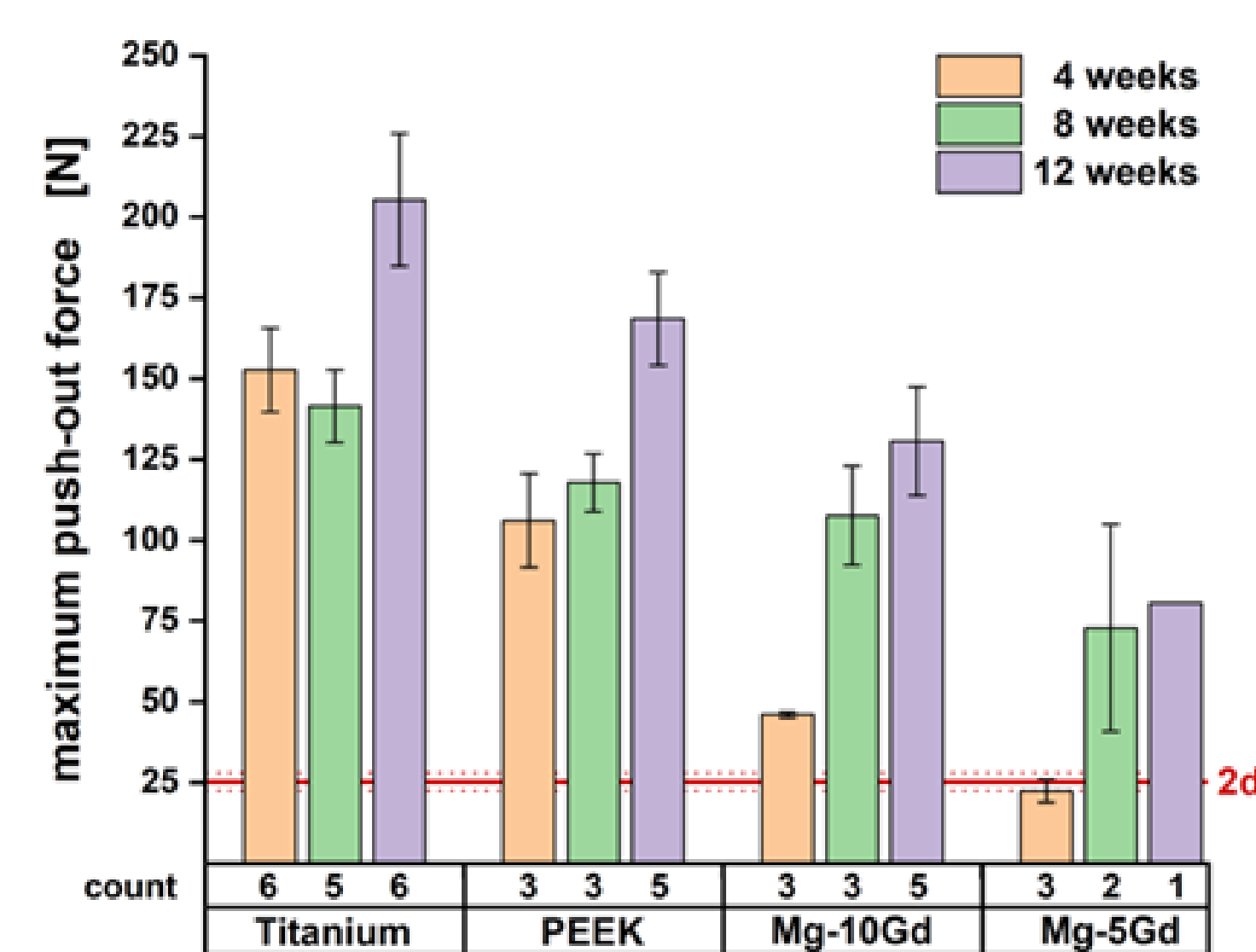


Figure 6: Expected value for the maximal applicable force to 1.9 mm o.d. screw implants. Error bars denote the standard error of the mean. The red line provides a lower boundary for primary implant stability. It is the average applicable force of two Mg-5Gd implants explanted without sufficient time for healing after just two days.

## Radial Bone Volume Density

- Mg-Gd alloys affect the bone tissue on a **larger length scale than non-resorbable implants** (~700  $\mu$ m into the sample).
- Bulging tissue is found for titanium and PEEK near the implant interface whereas Mg-Gd alloys reliably produce a **minimum in BV/TV** in its vicinity.
- **Poor cellular adhesion with PEEK** results in a 25  $\mu$ m gap to the bone tissue and a reduction in BV/TV between the screw threads.

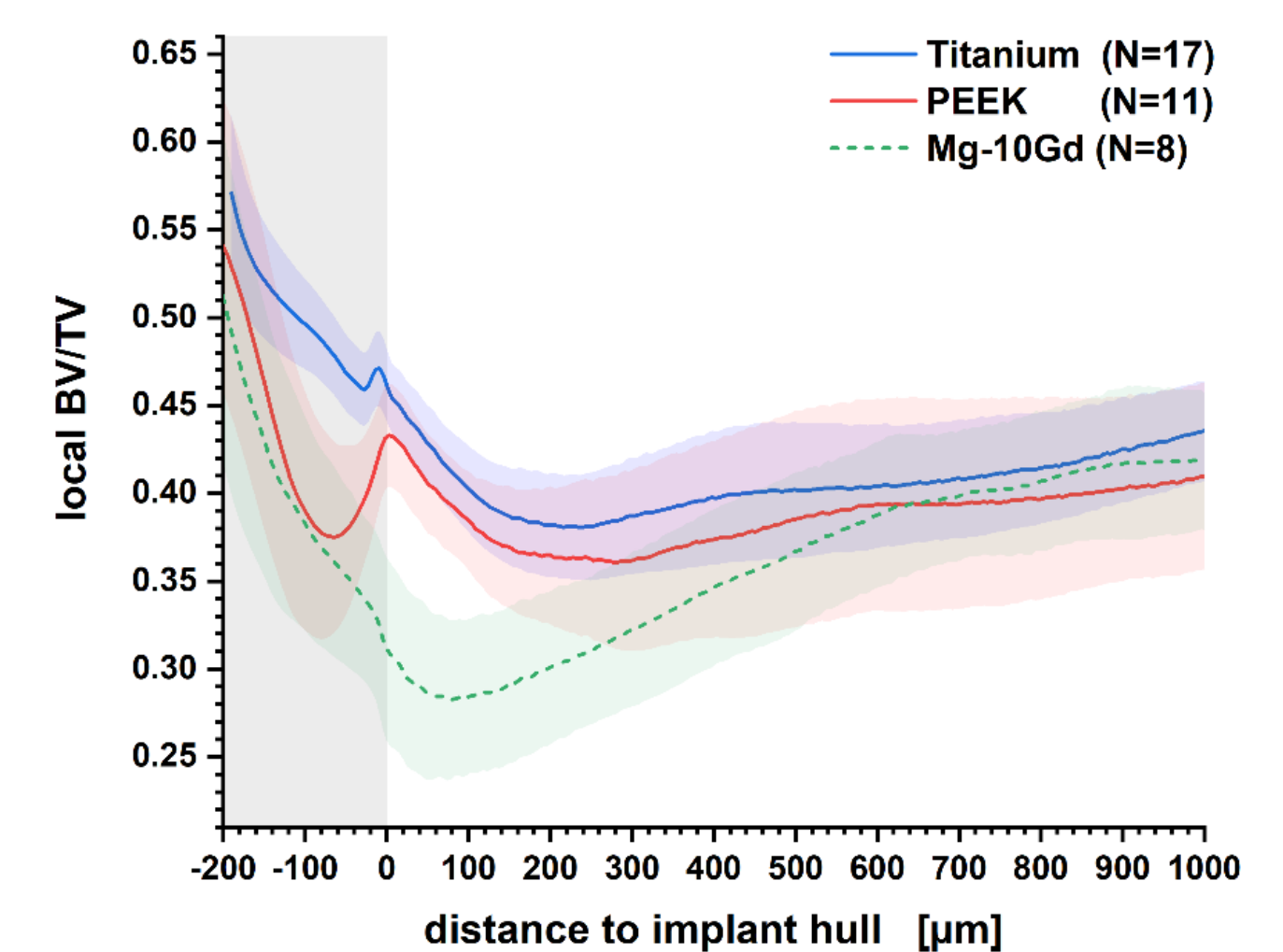


Figure 7: Radially resolved mean bone volume density for different implant materials depending on the Euclidean distance from the convex hull covering the implant. Colored shaded areas provide the t-score based 95% confidence interval, whereas the grey shade accentuates regions that are located between the screw threads.

## Strain Distribution

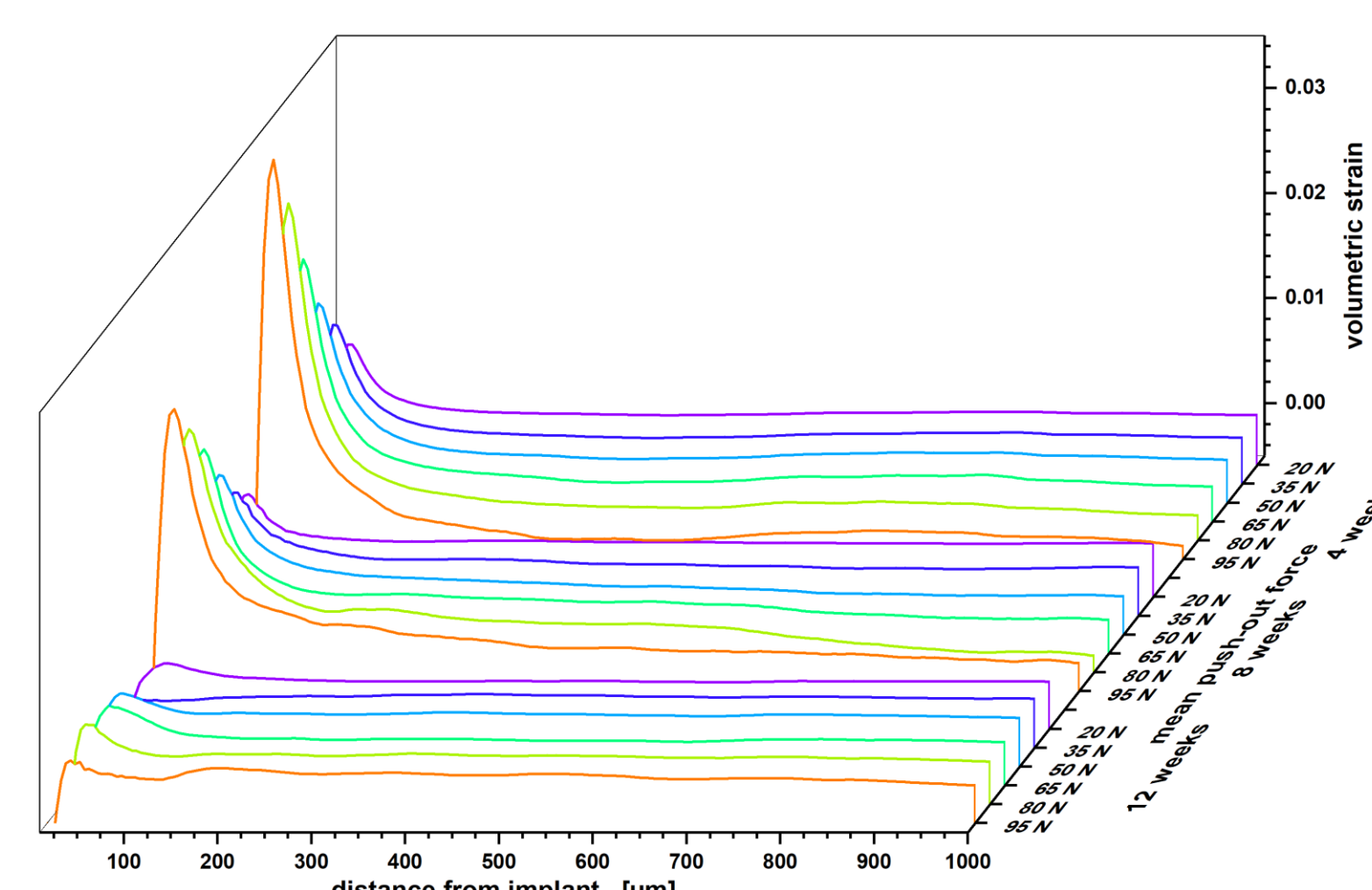
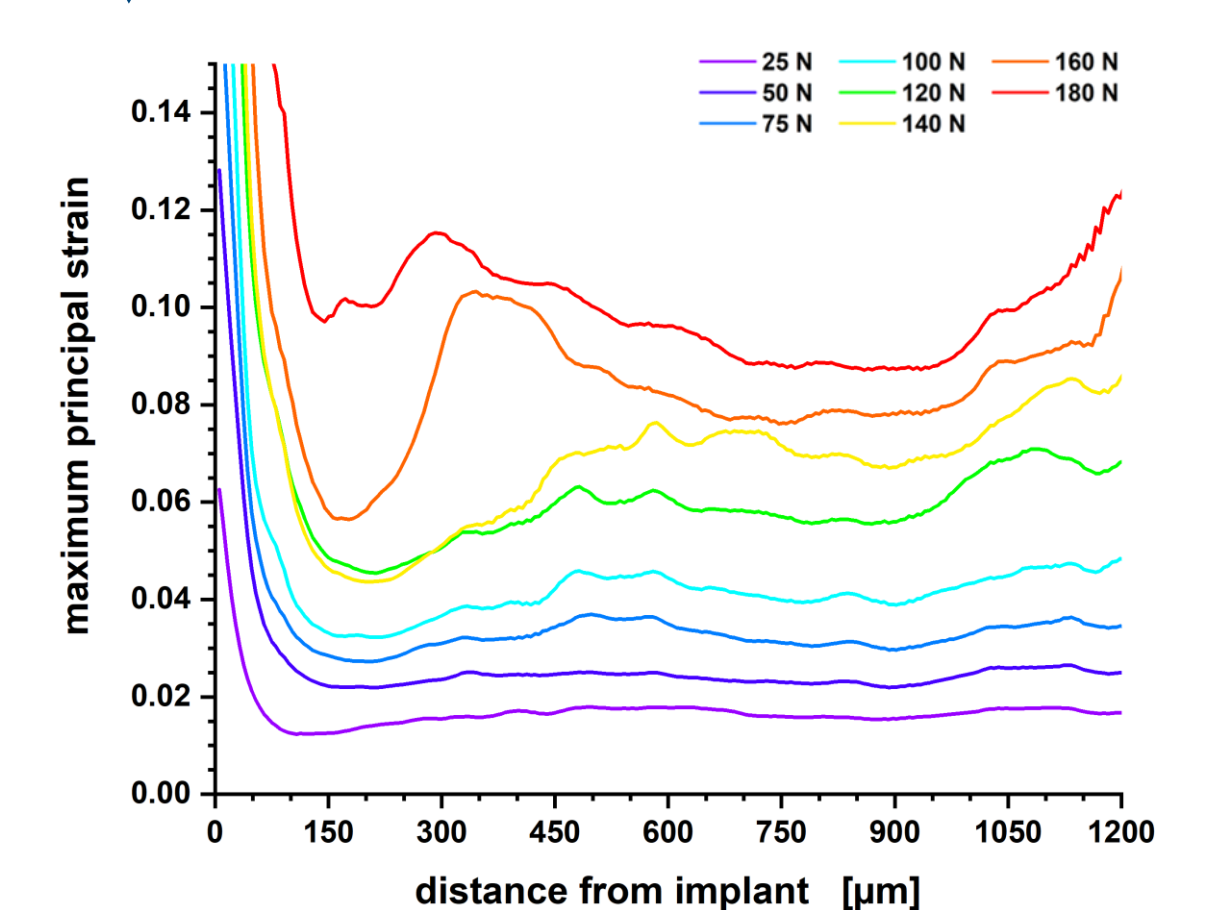


Figure 8: Mean volumetric strain for titanium implants with respect to varying healing period, material (row) and applied force during scan time (color).

Figure 9: Example for the high strain transfer with PEEK as an implant material showing the maximum principal strain for a sample after a 12 week healing period.



- Strain profiles **with titanium** as an implant material are **highly reproducible** with a maximum in strain 30  $\mu$ m from the implant.
- Limited contact and a compressible material with a Young's modulus close to bone results in **high strain transfer to the bone with PEEK** screws.
- Strain transfer with **Mg-xGd alloys** is reduced and **depends on the collapse of corroded material**.

